
Article:
Fekete, Marianna orcid.org/0000-0003-4869-0912, Ahwal, Fadi and Duckett, Simon B. orcid.org/0000-0002-9788-6615 (2020) Remarkable Levels of 15N Polarization Delivered through SABRE Into Unlabeled Pyridine, Pyrazine or Metronidazole Enable Single Scan NMR Quantification at the mM Level. Journal of Physical Chemistry B. jp-2020-02583e. ISSN 1520-5207

https://doi.org/10.1021/acs.jpcb.0c02583

THE JOURNAL OF PHYSICAL CHEMISTRY B

B: Liquids, Chemical and Dynamical Processes in Solution, Spectroscopy in Solution

Remarkable Levels of ^{15}N Polarization Delivered through SABRE Into Unlabeled Pyridine, Pyrazine or Metronidazole Enable Single Scan NMR Quantification at the mM Level

Marianna Fekete, Fadi Ahwal, and Simon B Duckett

J. Phys. Chem. B, **Just Accepted Manuscript** • DOI: 10.1021/acs.jpcb.0c02583 • Publication Date (Web): 08 May 2020

Remarkable levels of ^{15}N polarization delivered through SABRE into unlabeled pyridine, pyrazine or metronidazole enable single scan NMR quantification at the mM level.

*Marianna Fekete, Fadi Ahwal and Simon B. Duckett**

University of York, Department of Chemistry, Heslington, York, YO10 5DD (UK)

KEYWORDS. ^{15}N polarization, SABRE, *para*hydrogen

ABSTRACT. While many drugs and metabolites contain nitrogen, harnessing their diagnostic ^{15}N-NMR signature for their characterization is underutilized due to inherent detection difficulties. Here we demonstrate how precise ultra-low field SABRE (±0.2 mG) in conjunction *para*-hydrogen and an iridium precatalyst of the form IrCl(COD)(NHC) with the co-ligand d_9-benzylamine allows the natural abundance ^{15}N NMR signatures of pyridine, pyrazine, metronidazole and acetonitrile to be readily detected at 9.4 T in single NMR observations through >50% ^{15}N polarization levels. These signals allow rapid and precise reagent quantification via a response that varies linearly over the 2 mM to 70 mM concentration range.

Introduction

Hyperpolarization methods have been shown to dramatically improve the sensitivity of Nuclear Magnetic Resonance (NMR) and Magnetic Resonance Imaging (MRI)[1-2] in a process that involves increasing the purity of the magnetic states they detect. Signal amplification by reversible exchange (SABRE) reflects one such method. It harnesses the nuclear spin order of *para*-hydrogen (p-H_2)[3,4,5] and is a consequence of the pioneering work of Weitekamp[6] and Eisenberg.[7] For SABRE to operate, the symmetry of p-H_2 is first broken by temporarily placing it into a metal complex so that the new hydride ligands which result couple distinctly to NMR active spins within the ligand sphere of the product. A process of reversible binding then allows a suitable substrate to become hyperpolarized through what is a catalytic process that transfers nuclear spin order within the complex rather than achieving a change in chemical identity.[3,5] Typically this process takes place in a specified magnetic field that is often called the polarization transfer field (PTF) and can be selected to optimize efficiency.[8-9] The selection of this field is made according to the chemical shift difference that exists between the interacting nuclear spins and their spin-spin couplings[10,11] in a process that has been accurately modelled.[12] As the active SABRE catalyst may break the symmetry of the two protons that were initially located in p-H_2 through chemical or magnetic inequivalence effects the process of catalysis can be complex.[5, 13] This is because for spin order transfer from the p-H_2 derived hydride ligands to take place, the receiving ligand nuclei must exhibit different spin-spin couplings to these two protons.

Knowledge of this behavior has influenced SABRE catalyst design[14] and the resulting sensitization process has enabled the easy NMR detection of low-abundance inorganic species.[13] Other studies have used deuterated co-ligands to improve the spin-order yields in SABRE by

reducing waste through the focusing of polarization transfer into fewer receptor sites.[15] When this is achieved in conjunction with ^{2}H labelling, the associated extension of nuclear spin-order lifetime has proven to be particularly beneficial as de-coherence within the SABRE catalyst reflects one route to reduce the overall processes efficiency.[16] These two effects combine to extend the duration over which signals remain visible to NMR. as in classical terms one T_1 period is associated with a 63% destruction of the hard-won polarization level. Not surprisingly, the extended lifetimes associated with molecular singlet states[17-21] and their derivatives, feature extensively in hyperpolarization research as one goal is often to study *in vivo* reactivity.[22] In further developments, Tessari *et* al. have shown how ^{1}H-SABRE can achieve precise analyte quantification at low substrate loadings by the involvement of a slow exchanging co-ligand.[23-24] Furthermore, Iali *et* al extended SABRE to the hyperpolarization of primary amines through catalysts of the form $[Ir(H)_2(IMes)(amine)_3]Cl$,[25] and it was noted that sterically hindered amines which failed to bind efficiently benefited by the addition of smaller NCMe which enables the formation of $[Ir(H)_2(IMes)(aniline)_2(NCMe)]Cl$.[26] The successful use of amines reflects an important boost to SABRE because the hyperpolarized NH response can be used to sensitize other molecules through proton exchange.[25] More recently developments of this ligand design route have enabled the hyperpolarization of pyruvate and acetate.[27-28]

Normally, though the detection of ^{15}N by NMR is even more challenging than that of ^{1}H because of its 0.36% natural abundance and low magnetogyric ratio. ^{15}N detection is, however, needed for the characterization of important nucleobases, nucleosides, nucleotides, peptides, proteins and transition metal complexes. In addition, as the T_1 of ^{15}N can exceed many minutes, magnetic state lifetimes can approach those of positron emission tomography.[29-33] It is not therefore surprising that ^{15}N hyperpolarization reflected an early target of both spontaneous[3] and radio frequency

driven SABRE.[34] Warren *et* al. refined these methods through SABRE SHEATH[35-36] to deliver 20% ^{15}N polarization in metronidazole.[37] Several alternative radio frequency strategies have also been exemplified[38-40] and given the goal of *in vivo* SABRE, water soluble SABRE catalysts have also been described[41-42] with the MRI detection of a ^{15}N response illustrated.[42] Here though we seek to demonstrate how amines as co-ligands can enable the highly efficient ^{15}N polarization of a range of target substrates (sub) via SABRE catalysis through $[Ir(H)_2(\mathbf{1})(sub)_2(BnNH_2)]Cl$ (**a**) or $[Ir(H)_2(\mathbf{1})(sub)(BnNH_2)_2]Cl$ (**b**) of Scheme 1 in order to improve on the potential of SABRE approach to achieve *in vivo* MRI detection.

Results

Hyperpolarization of the ^{15}N NMR signal of pyridine.

We start by considering non-labelled pyridine at a 35 mM concentration because of its wide use in early SABRE research[3,4, 13] in conjunction with the precatalyst $[IrCl(COD)(h_{22}\text{-}\mathbf{1})]$[43] (5 mM) of Scheme 1. Our experimental measurements involved examining an NMR tube containing methanol-d_4 solutions of these reagents under 3 bar (absolute) pressure of p-H_2 at 99% purity. The p-H_2 gas is first dissolved by shaking the NMR tube whilst it is located in a pre-set magnetic field that lies between ±1 mG to ±140 G for ~10 seconds (relative to the main NMR magnets field orientation). Subsequently, the sample is placed in a 9.4 T magnet where the final NMR signal detection step occurs.

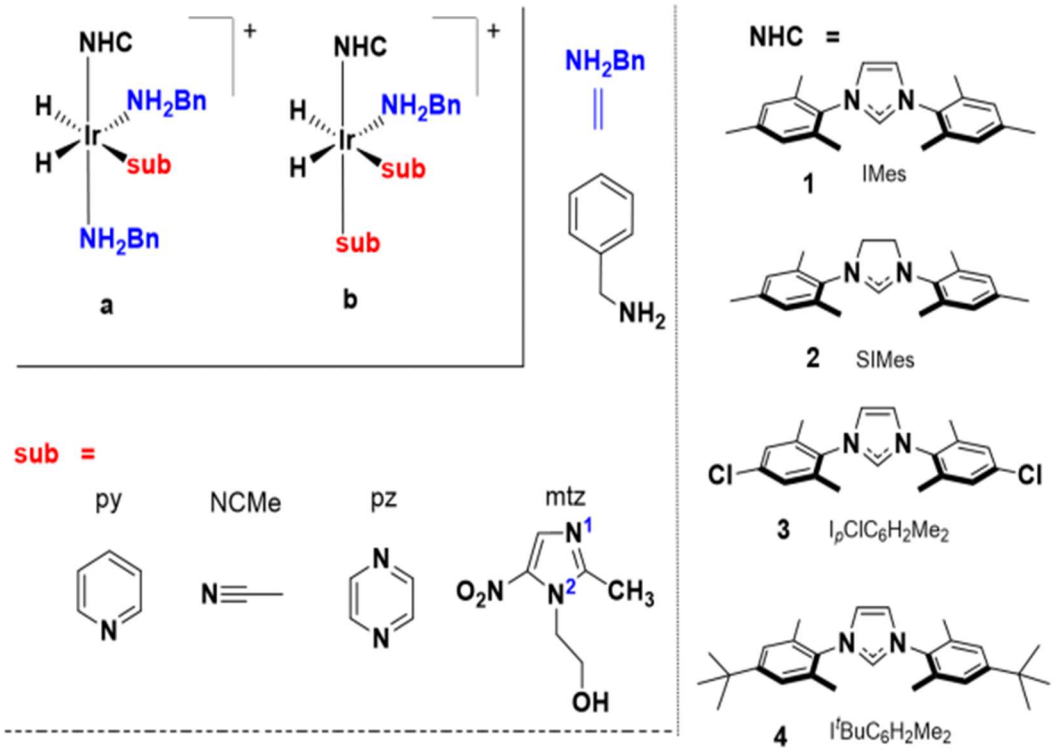

Scheme 1. Chemical structures of complexes, substrates and ligands.

Under these conditions, the SABRE catalyst $[Ir(H)_2(h_{22}\text{-}\mathbf{1})(py)_3]Cl$ forms and a ^1H NMR signal gain of 1452-fold can be seen for the *ortho*-proton resonance of free pyridine that is present in solution after transfer from a 60 G field. This polarization transfer step takes 10 seconds to complete and the resulting polarization level (P_H) is 4.65% (P_x reflects the percentage polarization associated with nuclei x). In this case, the catalyst breaks the symmetry of the two *p*-H_2 derived protons through magnetic inequivalence effects and hence spin order transfer flows optimally within the equatorial plane that contains the hydride ligands into bound pyridine.[44] For ^{15}N, however, the large *trans* two bond ^1H-^{15}N coupling of ~19 Hz[45,9,35, 46] that connects these hydride ligands to nitrogen in $[Ir(H)_2(h_{22}\text{-}\mathbf{1})(py)_3]Cl$ enables the efficient transfer of polarization at an approximate -1 mG field that is of the same sense to the main 9.4 T observation field. The

consequence of this process is a 39200 fold (±2%) ^{15}N-NMR signal gain which means the corresponding P_{15N} value is 12.9% (±2%). Hence this unlabeled 35 mM sample of pyridine can be detected by ^{15}N NMR spectroscopy in a single scan NMR measurement at a magnetic field of 9.4 T with a signal to noise ratio 11 using a routine inverse detection probe.

Establishing that the co-ligand benzylamine is beneficial to the hyperpolarization of the ^{15}N NMR signal of pyridine.

When the co-ligand d_7-benzylamine (d_7-$BnNH_2$) was added to such a sample, at an initial concentration of 17.5 mM, it proved to rapidly convert into its d_9-benzylamine isotopologue. Consequently, we refer to d_9-$BnND_2$ throughout this manuscript even though d_7-$BnNH_2$ is actually added to the samples. The resulting ^{1}H NMR spectra reveal that in addition to this labelling change, two new inorganic species are formed which yield pairs of hydride ligand signals at δ -22.14 and -22.58, and δ -23.34 and -23.73 respectively. These hydride ligand signals arise from $[Ir(H)_2(h_{22}$-**1**$)(d_9$-$BnND_2)(py)_2]Cl$ and $[Ir(H)_2(h_{22}$-**1**$)(d_9$-$BnND_2)_2(py)]Cl$ respectively that are present in solution in the ratio 2.6 : 1. The two complexes contain inequivalent hydride ligands that differ from one another according to the identity of the axial ligands in the complex as detailed in Scheme 1 and the SI. Furthermore, as their proportions match the value seen when a similar sample is created by the initial addition of benzylamine and H_2 to [IrCl(COD)(h_{22}-**1**)], but before pyridine addition takes place, it can be concluded that these two complexes are in equilibrium. Hence the separation of their roles in the underlying SABRE process is impractical, but we note it would be expected that both will contribute to this process. In addition, it is important to recognize that both of these complexes contain chemically and magnetically distinct hydride ligands. The result of this change is that spin-order transfer can now proceed into ligands that lie *trans* and *cis* to hydride, which means that spin dilution, associated with polarization of the axial ligands, is expected and

this will reduce the SABRE signal gains that are seen for the free substrate.[44] Hence, the involvement of polarization transfer protecting d_9-BnND$_2$ which limits spin-order wastage should be of significant benefit to the SABRE outcome.

When the resulting d_9-BnND$_2$ solutions were examined for SABRE, the ^{1}H NMR response resulting from this mixture of catalysts proved to contain a free pyridine *ortho* proton resonance that was 880-fold (± 50) larger than expected after transfer from a 60 G field. As this gain is smaller than the value achieved by [Ir(H)$_2$(h_{22}-**1**)(py)$_3$]Cl we can conclude that under these conditions the [Ir(H)$_2$(h_{22}-**1**)(d_9-BnND$_2$)(py)$_2$]Cl/[Ir(H)$_2$(h_{22}-**1**)(d_9-BnND$_2$)$_2$(py)]Cl mixture is actually less efficient at hyperpolarizing the ^{1}H NMR signals of pyridine than [Ir(H)$_2$(h_{22}-**1**)(py)$_3$]Cl. More notable though is the fact that the corresponding ^{15}N NMR spectrum contains a signal that is indicative of a P_{15N} value of 18% (53300 ± 6000 fold) in conjunction with a PTF of approximately -1 mG (Figure 1a). This reflects a 27% improvement in SABRE efficiency when compared to that achieved by [Ir(H)$_2$(h_{22}-**1**)(py)$_3$]Cl and confirms that there is a benefit to using the co-ligand d_9-benzylamine when seeking ^{15}N polarization.

Upon changing to [IrCl(d_{22}-**1**)(COD)], and completing a similar series of d_9-BnND$_2$ promoted measurements, the levels of signal gain seen in the pyridine *ortho* proton ^{1}H NMR signal rises to 1324-fold, although the ^{15}N polarization level proved to be unaffected. Hence, while catalyst deuteration is not successful at improving SABRE ^{15}N activity, it is able to improve the level of ^{1}H signal gain because of reduced spin order wastage and improved ^{1}H relaxation.[16] This suggests that low-field ^{15}N-relaxation within the catalyst is not improved.

While it is well known that the optimum SABRE catalyst changes with the identity of the substrate, it has been clearly demonstrated here that there is also a further dependence on the

efficiency of SABRE transfer within a given substrate according to whether ^{1}H or ^{15}N is the target. The optimum rate of ligand exchange for ^{1}H transfer has been proposed by Barskiy to be 4.5 s^{-1} in complexes of the type $[Ir(H)_2(h_{22}\text{-}\mathbf{1})(py)_3]Cl$. Consequently, the rate of pyridine substrate dissociation in $[Ir(H)_2(h_{22}\text{-}\mathbf{1})(py)_2(d_9\text{-}BnND_2)]Cl$ in methanol-d_4 solution was determined using the EXSY method and found to be 0.06 s^{-1} at 268 K. This value increases to 1.04 s^{-1} upon warming to at 298 K, and 2.1 s^{-1} at 308 K. Our associated SABRE measurements reveal that the corresponding ^{1}H NMR signal gains change from 600-fold, through 4530-fold to 3550-fold at the 308 K setting. Hence it appears that a rate closer to 1.04 s^{-1} is optimal for ^{1}H transfer into pyridine using this catalyst. Our experiments also reveal that there is a 30% growth in efficiency of ^{15}N polarization for pyridine on moving from 268 K to 298 K, and a further 22% improvement on moving to 308 K from 298 K. Consequently, we can confirm that the two different nuclei are best served with different rates of ligand exchange.

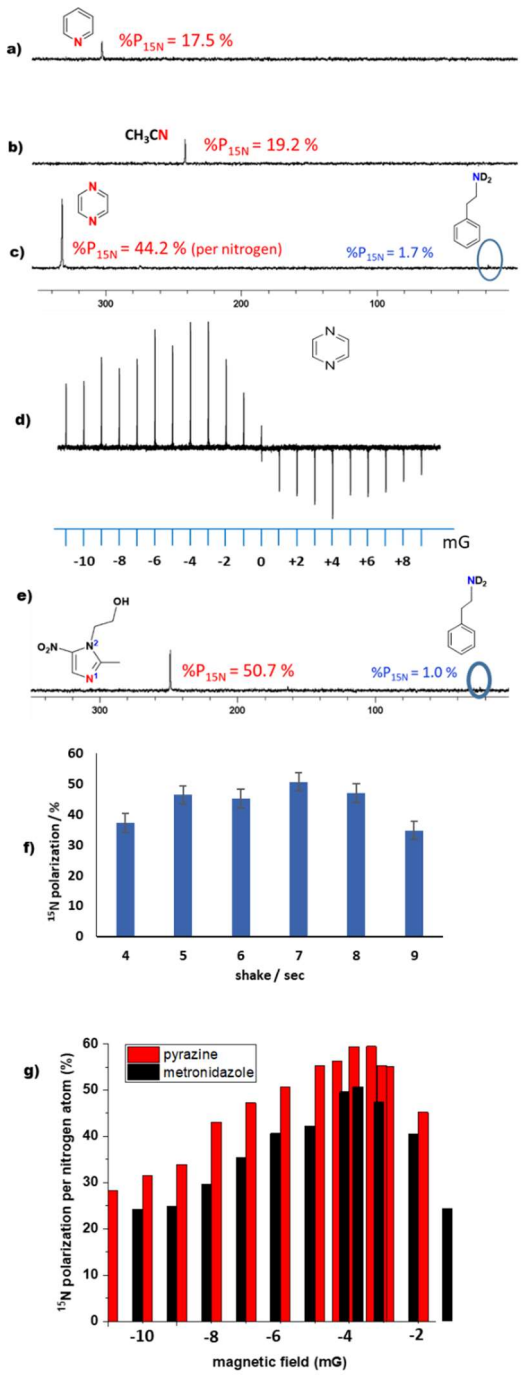

Figure 1. Polarized ^{15}N NMR signals of a) pyridine, b) acetonitrile, c) and d) pyrazine and e) metronidazole. Levels indicted in figure alongside agent. In d), the series of ^{15}N NMR signals for pyrazine vary in intensity according to the magnitude of the polarization transfer field. f) Shake time dependence of P_{15N} level in metronidazole with [IrCl(d_{34}-**4**)(COD)]. g) P_{15N} level for metronidazole (black) and pyrazine (red) in a 10 mm sample tube as a function of PTF magnitude.

Hyperpolarization of the ^{15}N NMR signal of acetonitrile.

In order to develop this method further, acetonitrile was tested at a similar 35 mM concentration in conjunction with the SABRE catalyst [Ir(H)$_2$(h_{22}-**1**)(NCMe)$_3$]Cl. This catalyst also relies on magnetic inequivalence to break the symmetry of the hydride ligands and it yields a ^{1}H NMR signal gain of just 83-fold per methyl proton in the unbound acetonitrile present in solution after transfer at 298 K from a 70 G field. The SABRE derived ^{15}N NMR signal gain for CH_3CN was found to be far more substantial, at 41800 ± 6000 fold (14% polarization) after transfer from an approximate -1 mG field.

Acetonitrile hyperpolarization was then studied in conjunction with 3.6 equivalents of the co-ligand d_9-benzylamine relative to a 5.2 mM iridium concentration. Both [Ir(H)$_2$(d_9-BnND$_2$)$_2$(NCMe)(h_{22}-**1**)]Cl and [Ir(H)$_2$(d_9-BnND$_2$)$_3$(h_{22}-**1**)]Cl form in these experiments, in a 2:1 ratio. They both possess chemically distinct hydride ligands. The resulting ^{1}H NMR response after SABRE showed an improved ^{1}H NMR signal gain of 160-fold per proton for CH_3CN while its ^{15}N polarization level rose to 19% (Figure 1b).

For the corresponding ^{2}H labeled precatalyst [IrCl(d_{22}-**1**)(COD)], the ^{1}H NMR signal again improves further to 367-fold per proton in accordance with reduced spin dilution that arises as a consequence of hydride ligand chemical inequivalence in [Ir(H)$_2$(d_9-BnND$_2$)$_2$(NCMe)(h_{22}-**1**)]Cl and [Ir(H)$_2$(d_9-BnND$_2$)$_3$(h_{22}-**1**)]Cl, but now the achieved P_{15N} level fell to 10%. Hence ^{2}H-catalyst labelling of the NHC ligand is now detrimental to the ^{15}N polarization level. In this case, the appreciable concentration of [Ir(H)$_2$(d_9-BnNH$_2$)$_2$(NCMe)(d_{22}-**1**)]Cl, where there will be coupling between the ^{2}H labels of the NHC and the ^{15}N of NCMe, could result in the reduction in ^{15}N-SABRE efficiency. Barskiy's observations that in micro-Tesla transfer fields scaler relaxation of

the second kind[47] associated with the quadrupolar ^{14}N-^{13}C interaction limits the level of ^{13}C polarization under SABRE support this view.[48] The gain in ^{1}H signal intensity relative to the situation with h_{22}-**1** is, however, consistent with a reduction in polarization transfer into this ligand through deuteration and an extension of the hydride ligands relaxation times.[14]

Hyperpolarization of the ^{15}N NMR signal of pyrazine.

We next consider pyrazine (pz). This substrate was tested by taking 5.2 mM methanol-d_4 solutions of [IrCl(COD)(h_{22}-**1**)] that contained a 7-fold excess of pz under 3 bar of p-H_2. The resulting ^{1}H NMR signal gain for pz was now 900 fold per proton (2.9 % polarization) and a P_{15N} value of 16% (± 2, per nitrogen used throughout) was observed after transfer from -3mG.

Studies with added h_7-$BnND_2$ resulted in a ^{1}H NMR signal gain of 566 fold (0.8%) and a ^{15}N signal gain of 12% due to the associated spin dilution effects. However, when d_9-$BnND_2$ and h_{22}-1 were used with a PTF of 60 G, radiation damping resulted with ^{1}H signal detection. In order to aid the analysis, this artifact could be suppressed if a less efficient PTF of 120 G was used. Analysis under these conditions was used to deduce that the corresponding P_H level is 13.5% (± 0.6) per proton for a 60 G measurement while for ^{15}N it was 38% (per nitrogen). The ^{1}H NMR signal gain grew further to 30.9% (± 0.7) when [IrCl(d_{22}-**1**)(COD)] was used but the corresponding ^{15}N signal response fell in intensity meaning that scaler relaxation of the second kind is again important We also tested the related SIMes containing precatalyst [IrCl(COD)(**2**)][49] with pyrazine and discovered that a P_{15N} value of 15.8% could be achieved without a co-ligand. Samples containing both d_7-benzylamine and pyrazine yield [$Ir(H)_2(pz)_2$(d_9-$BnND_2$)(h_{22}-**2**)]Cl and [$Ir(H)_2$(d_9-$BnND_2)_2$(pz)(h_{22}-**2**)]Cl in the ratio 2:1 and a P_{15N} value of 44.2% via PTF from an approximate -1.9 mG field (Figure 1c). This falls to 31.8% with d_{22}-SIMes in agreement with a role for ^{2}H-drive

relation in the SABRE catalyst at low field. Figure 1d shows that the sign of the polarization transfer field, relative to that of the main observation field affects the measured ^{15}N pz signal gains. This is because upon moving the sample slowly between the points of polarization transfer and measurement if it experiences a zero-field point there is a loss in spin order due to relaxation at this point.

The rate of pyrazine dissociation from [Ir(H)$_2$(pz)$_2$(d_9-BnND$_2$)(h_{22}-**2**)]Cl was determined using the EXSY method to be 0.33 s^{-1} at 268 K when the ^{1}H NMR signal gain is 660 fold. This rate increases to 1.8 s^{-1} at 298 K where the ^{1}H signal gain is 2200 fold. Our experiments reveal a 20% growth in efficiency of ^{15}N polarization on moving from 268 K to 298 K for pyrazine as a consequence of this rate increase which is faster than that of pyridine loss in the related complex [Ir(H)$_2$(h_{22}-**1**)(py)$_2$(d_9-BnND$_2$)]Cl. This kinetic difference is consistent with the relative ^{15}N polarization efficiencies of 44.2% and 18% respectively.

Hyperpolarization of the ^{15}N NMR signal of metronidazole.

Biologically significant metronidazole[50, 51] has been well-studied by Chekmenev *et al.*[52, 53, 54, 55] We conducted control measurements for 5.2 mM methanol-d_4 solutions of [IrCl(COD)(h_{22}-**1**)] and [IrCl(COD)(h_{22}-**2**)] with a 7-fold excess of metronidazole relative to iridium and a 3 bar pressure of *p*-H$_2$ but failed to see significant polarization in either sample. However, once a 3.6-fold excess of d_7-benzylamine was added, polarization transfer to proton and ^{15}N was readily seen with both precursors. For [IrCl(COD)(h_{22}-**1**)] the P_{15N} value was 22% whilst for [IrCl(COD)(h_{22}-**2**)] it was 24% (transfer at -2 mG and 2% P_{15N} seen for d_7-benzylamine itself). When the ^{2}H labeled versions of these catalysts, [IrCl(COD)(d_{22}-**1**)] or [IrCl(COD)(d_{22}-**2**)], were used, these P_{15N} values rose to

27%. In all cases the reaction with d_9-benzylamine and metronidazole formed [Ir(H)$_2$(mtz)$_2$(d_9-BnND$_2$)(NHC)]Cl and [Ir(H)$_2$(d_9-BnND$_2$)$_2$(mtz)(NHC)]Cl with the ratio being 1.4:1 for d_{22}-**2**.

Data was now collected on the d_{22}-**2** system to demonstrate that the PTF value can be used to control which of the two substrates present in solution receives polarization. This effect serves to illustrate how selectivity can be introduced into the analysis of mixtures if peak overlap is an issue (see SI). Furthermore, a catalyst change to [IrCl(COD)(d_{34}-**4**)] increased the N_1 value to 51% for metronidazole with 4% polarization being achieved on N_2 and 1% on d_9-benzylamine.

The rates of metronidazole dissociation from the resulting complex [Ir(H)$_2$(mtz)$_2$(d_9-BnND$_2$)(d_{34}-**4**)]Cl were determined in methanol-d_4 solution at 268, 298 and 308 K by the EXSY method as being 0.80 s^{-1}, 2.37 s^{-1} and 5.5 s^{-1} respectively. For the ^{1}H signal gain, 298 K proved to be best, yielding an enhancement of 856-fold. We now see an 80% growth in efficiency of ^{15}N polarization on moving from 268 K to 298 K, but the P_{15N} values falls to just 18% at 308 K. Hence increasing the ligand exchange rate beyond 2.4 s^{-1} seems detrimental.

	Nucleus (PTF) / Signal Gain (P)	1	d_{22}-1	2	d_{22}-2	3	d_{16}-3	4	d_{34}-4	Error, %, ±
Pyrazine	^{1}H (120 G) / fold	1372	3151	2220	6028	2533	558	556	673	4
	^{15}N (%, as indicated PTF mG)	38 (-3)	35 (-3)	44 (-1.9)	37 (-5)	26 (-2)	31 (-4)	32 (-5)	28 (-3)	2
Metronidazole-N$_1$	^{1}H (60 G)/ fold	326	474	560	446	814	1038	676	856	5
	^{15}N(%, at PTF of -2 mG)	22	27	24	27	23	23	32	51	3

Table 1. Absolute value of ^{1}H (total proton) and ^{15}N NMR (per site) signal enhancement levels for pyrazine and metronidazole at the specified PTF for samples with d_9-benzylamine as a co-ligand.

Using higher proportions of *p*-H_2 to improve the NMR signal gain.

A series of measurements were then completed on metronidazole using a 10 mm NMR tube to deploy a larger excess of *p*-H_2 in conjunction with [IrCl(COD)(d_{34}-**4**)] and d_9-benzylamine. A slight increase in ^{15}N polarization level to 54% results alongside a reduction in response variability to 2%. Consequently, as shown in Figure 1g, a -3.6 mG PTF can be deduced as being optimal. Similar 10 mm measurements were then made for pyridine with [IrCl(COD)(h_{22}-**1**), acetonitrile with [IrCl(COD)(h_{22}-**1**) and pyrazine with [IrCl(COD)(h_{22}-**2**) in the presence of d_9-benzylamine. These studies saw the P_{15N} level for pyridine increase to 48% at 4 bar *p*-H_2 pressure. When acetonitrile was examined a 30.7% P_{15N} level was reached, but for pyrazine it became 59.4% per nitrogen. Further increases in the pyrazine % P_{15N} level can be achieved through reagent dilution such that when an initial 5 mM solution of [IrCl(COD)(h_{22}-**2**)] with a 3.6-fold excess of d_9-benzylamine and 7-fold excess of pyrazine based on iridium is diluted 10 fold, the P_{15N} value increases to 79%; the S/N ratio in this case is 11.3. In this case the effect is directly analogous to increasing the volume of *p*-H_2 available.

Quantification of reagent concentrations at the mM level through a SABRE enhanced ^{15}N signal

Once we had ascertained how to achieve these polarization levels, we tested how the magnitude of the pyridine, pyrazine and metronidazole response varied as a function of substrate concentrations between 2.2 and 70 mM. These solutions were made up by simply diluting a stock solution with an initial catalyst, d_7-benzylamine and substrate concentration of 10 mM, 36 mM and 70 mM respectively. We discovered that there was a linear variation in signal response is each case as detailed in Figure 2.

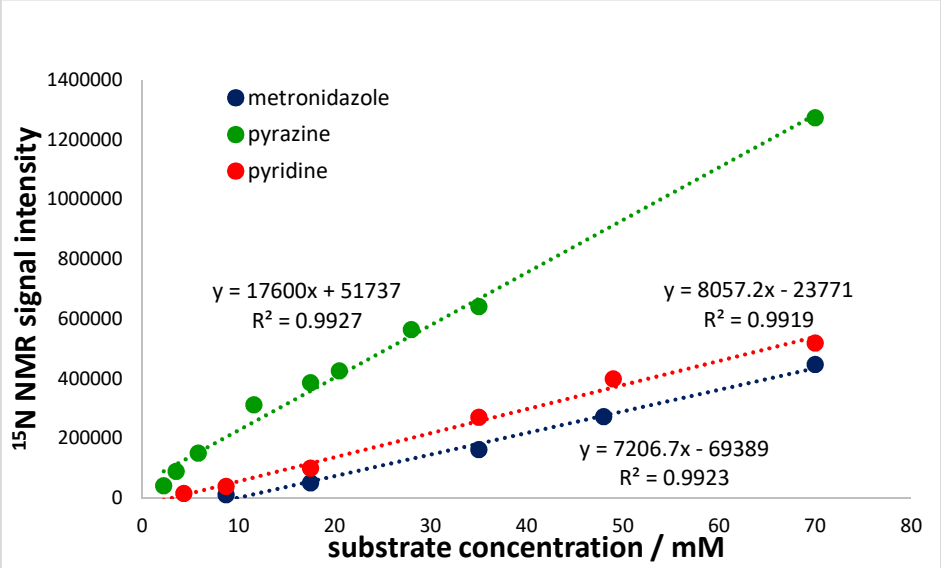

Figure 2. Raw signal intensity resulting from a series of hyperpolarized ^{15}N NMR spectra of pyridine, metronidazole and pyrazine as a function of their concentration. The polarization transfer field was optimized for each substrate. The stock solution of the sample ([Ir] = 6.5mM, substrate = 70 mM, and 22.7 mM d_9-BnND$_2$) was diluted during these measurements, from 70 mM substrate to 2.2 mM substrate concentration. The straight lines result from linear regression analysis and the square of the sample correlation coefficient -R^2-confirms linear behavior.

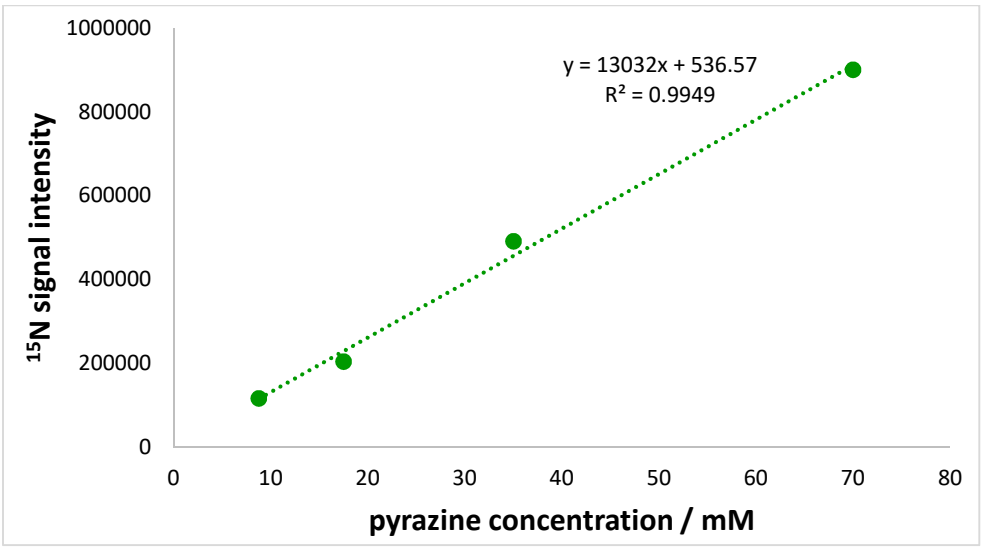

Figure 3. Raw signal intensity resulting from a series of hyperpolarized ^{15}N NMR spectra of pyrazine as a function of its concentration. The polarization transfer field used was -1.9 mG. The concentration of the [Ir]-precatalyst ([IrCl(COD)(h_{22}-**2**)]) was kept constant at 6.5 mM. 3.6 equivalents of d_9-BnND$_2$ were added relative to metal. Subsequently, the concentration of added

pyrazine was varied from 8.2 mM to 70 mM. Straight line behavior results thereby confirming that the absolution concentration of pyrazine can be estimated from such data.

In second series of studies we maintained a constant iridium and co-ligand concentration whilst changing the pyrazine concentration. A linear change in ^{15}N signal intensity was again observed (Figure 3) despite in this case observing some changes in catalyst form. The hydride region of the polarized NMR spectra confirm that both [Ir(H)$_2$(pz)(d_9-BnND$_2$)$_2$(h_{22}-**2**)]Cl (**A**) and [Ir(H)$_2$(pz)$_2$(d_9-BnND$_2$)(h_{22}-**2**)]Cl (**B**) of Figure 4 form with the former being favored at low pyrazine loadings. As the concentration of pyrazine decrease, the amount of the formed complex **B** decreases and as a result of it the ^{15}N polarization of pyrazine linearly decrease as well. This suggest that the main SABRE – ^{15}N catalyst is the type **B** complex. We are currently exploring this behavior in more detail. These data therefore confirm that substrate detection and quantification is feasible via a ^{15}N SABRE signal (see SI).

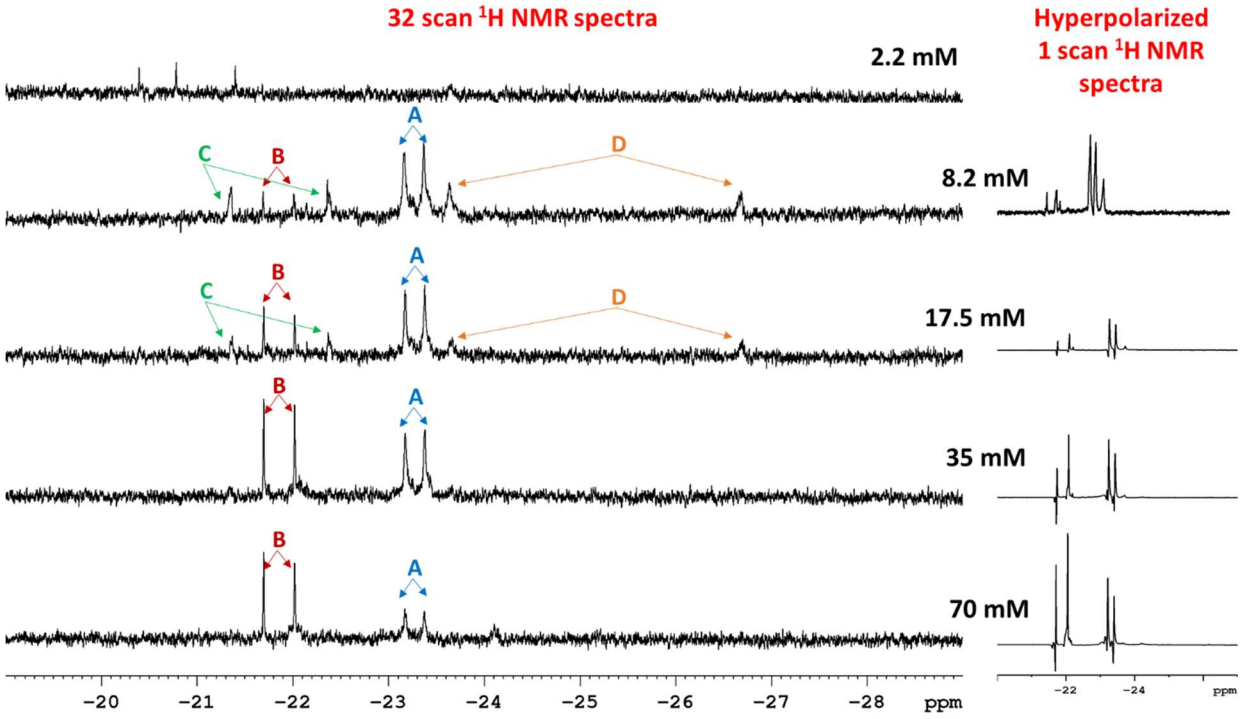

Figure 4: Effect of pyrazine loading on catalyst speciation when methanol-d_4 solutions of [IrCl(COD)(h_{22}-**2**)] are examine with d_9-BnND$_2$ and pyrazine in the presence of p-H$_2$ seen through the hydride region of the corresponding ^{1}H NMR spectra. Left, thermally equilibrated NMR spectra, right initial SABRE enhanced NMR spectra. Species **A** and **B** are defined in the text whilst **C** is Ir(H)$_2$(Cl)(d_9-BnND$_2$)(pz)(h_{22}-**2**) and **D** [Ir(H)$_2$(d_9-BnND$_2$)(methanol-d_4)(h_{22}-**2**)]Cl.

Conclusions

We have described here how the addition of the co-ligand d_9-benzylamine to a precatalyst based on [IrCl(NHC)(COD)] under p-H$_2$ results in very high levels of ^{15}N polarization in a range of substrates. The high field measurements were made in conjunction with the simple shake and drop approach, and it takes approximately 17 seconds to complete a measurement. In the case of the substrates pyridine and acetonitrile, [IrCl(h_{22}-**1**)(COD)] led to P_{15N} values of 48% and 30.9% respectively after transfer from an appropriate mG field. In contrast, a 59.4 P_{15N} value for pyrazine was achieved using the precatalyst [IrCl(h_{22}-**2**)(COD)]. These reactions involve the formation of a range of SABRE catalysts of the form [Ir(H)$_2$(sub)$_2$(d_9-BnND$_2$)(NHC)]Cl and [Ir(H)$_2$(sub)(d_9-BnND$_2$)$_2$(NHC)]Cl which are in equilibrium.

Previous studies have established that using deuterated NHC ligands (d_{22}-**1** and d_{22}-**2**) improve SABRE hyperpolarization transfer efficiency into methylnicotinate. This improvement is based on an extension of the hydride ligands relaxation times.[14] Studies here confirm that higher P_{1H} values result in all cases in support of this benefit. However, deuteration is not beneficial for ^{15}N transfer in pyridine, pyrazine and acetonitrile. Barskiy's observations that in micro-Tesla transfer fields scaler relaxation of the second kind[47] associated with the quadrupolar ^{14}N-^{13}C interaction limits the level of ^{13}C polarization under SABRE offer a route to explain this view.[48] For metronidazole,

however, an improved value of 54% on N_1 results with d_9-benzylamine and [IrCl(COD)(d_{34}-**4**)] which when compared to that seen with precatalyst [IrCl(COD)(h_{34}-**4**)]. Hence, ^{2}H labelling of the catalyst can also be of significant benefit to P_{15N}.

The rates of ligand exchange were also assessed alongside the collection of variable temperature SABRE data. It was found that the rate of optimum ligand exchange was slower than that found for ^{1}H transfer despite the larger ^{1}H-^{15}N transfer coupling. We are currently exploring this behavior in more detail.

Data was also presented that was collected from larger 10 mm NMR tubes using a 4 bar pressure of *p*-H_2. This acted to increase the relative excess of the hyperpolarization fuel *p*-H_2 relative to the substrate and proved to result in greatly improved response reproducibility. Consequently, results demonstrated that a polarization transfer field precision of ±0.2 mG is needed for optimal ^{15}N transfer. In addition, ~50% ^{15}N polarization levels could now be achieved in pyrazine, pyridine or metronidazole, which makes them all highly detectable even at low concentration.

In order to demonstrate an analytical use for these ^{15}N signals, results were presented to demonstrate that the magnitude of the resulting NMR response scales linearly with concentration over the range 2.2 to 70 mM. This means that such SABRE-derived data can be used to quantify their amount in solution when set against a suitable reference trace. Tessari have completed a growing range of studies which demonstrate ^{1}H detection levels can be linked to both speciation and quantity[23-24], while we have described how ^{13}C signals in glucose can be linked to amount.[56] These studies employed a methylated triazol co-ligand to simplify the exchange kinetics in order to produce the necessary linear response. We were unable to benchmark our data with that of the triazol co-ligand as it is not commercially available. We did, however, test d_6-dmso which is

finding widespread use as a co-ligand for the sensitization of weakly binding substrates as an alternative. As detailed in the SI the corresponding SABRE performance was degraded.

It is therefore clear that SABRE offers a simple and yet efficient route to analyte quantification by ^{15}N NMR spectroscopy. Not surprisingly, we predict these results will therefore be of benefit if you wish to use ^{15}N NMR as a characterization tool, or simply to quantify precise, and yet low, levels of nitrogen containing drugs that are present in solution or to collect ^{15}N-MRI data.

ASSOCIATED CONTENT

Supporting Information. Experimental details, NMR data and hyperpolarization details

AUTHOR INFORMATION

Corresponding Author

*Email for S. B. D.: simon.duckett@york.ac.uk

Author Contributions

The manuscript was written through contributions of all authors. All authors have given approval to the final version of the manuscript. ‡

Funding Sources

Financial support from the Wellcome Trust (Grants 092506 and 098335), the MRC (MR/M008991/1) and the University of York is gratefully acknowledged. **Notes**

Any additional relevant notes should be placed here.

ACKNOWLEDGMENT

We thank Peter Rayner for providing some of the complexes used in this work.

REFERENCES

1. Dumez, J. N., Perspectives on hyperpolarised solution-state magnetic resonance in chemistry. *Magn. Reson. Chem.* **2017,** *55* (1), 38-46.
2. Kovtunov, K. V.; Pokochueva, E. V.; Salnikov, O. G.; Cousin, S. F.; Kurzbach, D.; Vuichoud, B.; Jannin, S.; Chekmenev, E. Y.; Goodson, B. M.; Barskiy, D. A.; Koptyug, I. V., Hyperpolarized NMR Spectroscopy: d-DNP, PHIP, and SABRE Techniques. *Chem.-Asian J.* **2018,** *13* (15), 1857-1871.
3. Adams, R. W.; Aguilar, J. A.; Atkinson, K. D.; Cowley, M. J.; Elliott, P. I. P.; Duckett, S. B.; Green, G. G. R.; Khazal, I. G.; López-Serrano, J.; Williamson, D. C., Reversible Interactions with para-Hydrogen Enhance NMR Sensitivity by Polarization Transfer. *Science* **2009,** *323* (5922), 1708-1711.
4. Atkinson, K. D.; Cowley, M. J.; Elliott, P. I. P.; Duckett, S. B.; Green, G. G. R.; López-Serrano, J.; Whitwood, A. C., Spontaneous Transfer of Parahydrogen Derived Spin Order to Pyridine at Low Magnetic Field. *J. Am. Chem. Soc.* **2009,** *131* (37), 13362-13368.
5. Adams, R. W.; Duckett, S. B.; Green, R. A.; Williamson, D. C.; Green, G. G. R., A theoretical basis for spontaneous polarization transfer in non-hydrogenative parahydrogen-induced polarization. *Journal of Chemical Physics* **2009,** *131* (19), 194505.
6. Bowers, C. R.; Weitekamp, D. P., Transformation of symmetrization order to nuclear-spin magnetization by chemical-reaction and nuclear-magnetic-resonance. *Phys. Rev. Lett.* **1986,** *57* (21), 2645-2648.
7. Eisenberg, R., Parahydrogen-induced polarization - a new spin on reactions with H2. *Accounts Chem. Res.* **1991,** *24* (4), 110-116.
8. Dücker, E. B.; Kuhn, L. T.; Münnemann, K.; Griesinger, C., Similarity of SABRE field dependence in chemically different substrates. *J. Magn. Reson.* **2012,** *214*, 159-165.
9. Cowley, M. J.; Adams, R. W.; Atkinson, K. D.; Cockett, M. C. R.; Duckett, S. B.; Green, G. G. R.; Lohman, J. A. B.; Kerssebaum, R.; Kilgour, D.; Mewis, R. E., Iridium N-Heterocyclic Carbene Complexes as Efficient Catalysts for Magnetization Transfer from para-Hydrogen. *J. Am. Chem. Soc.* **2011,** *133* (16), 6134-6137.
10. Green, R. A.; Adams, R. W.; Duckett, S. B.; Mewis, R. E.; Williamson, D. C.; Green, G. G. R., The theory and practice of hyperpolarization in magnetic resonance using parahydrogen. *Progress in Nuclear Magnetic Resonance Spectroscopy* **2012,** *67*, 1-48.
11. Korchak, S. E.; Ivanov, K. L.; Yurkovskaya, A. V.; Vieth, H. M., Para-hydrogen induced polarization in multi-spin systems studied at variable magnetic field. *Phys. Chem. Chem. Phys.* **2009,** *11* (47), 11146-11156.
12. Barskiy, D. A.; Knecht, S.; Yurkovskaya, A. V.; Ivanov, K. L., SABRE: Chemical kinetics and spin dynamics of the formation of hyperpolarization. *Progress in Nuclear Magnetic Resonance Spectroscopy* **2019,** *114-115*, 33-70.

13. Fekete, M.; Bayfield, O.; Duckett, S. B.; Hart, S.; Mewis, R. E.; Pridmore, N.; Rayner, P. J.; Whitwood, A., Iridium(III) Hydrido N-Heterocyclic Carbene–Phosphine Complexes as Catalysts in Magnetization Transfer Reactions. *Inorg. Chem.* **2013,** *52* (23), 13453-13461.
14. Rayner, P. J.; Norcott, P.; Appleby, K. M.; Iali, W.; John, R. O.; Hart, S. J.; Whitwood, A. C.; Duckett, S. B., Fine-tuning the efficiency of para-hydrogen-induced hyperpolarization by rational N-heterocyclic carbene design. *Nature Communications* **2018,** *9* (1), 4251.
15. Fekete, M.; Rayner, P. J.; Green, G. G. R.; Duckett, S. B., Harnessing polarisation transfer to indazole and imidazole through signal amplification by reversible exchange to improve their NMR detectability. *Magn. Reson. Chem.* **2017,** *55* (10), 944-957.
16. Rayner, P. J.; Burns, M. J.; Olaru, A. M.; Norcott, P.; Fekete, M.; Green, G. G. R.; Highton, L. A. R.; Mewis, R. E.; Duckett, S. B., Delivering strong H-1 nuclear hyperpolarization levels and long magnetic lifetimes through signal amplification by reversible exchange. *Proc. Natl. Acad. Sci. U. S. A.* **2017,** *114* (16), E3188-E3194.
17. Roy, S. S.; Norcott, P.; Rayner, P. J.; Green, G. G. R.; Duckett, S. B., A Hyperpolarizable H-1 Magnetic Resonance Probe for Signal Detection 15 Minutes after Spin Polarization Storage. *Angew. Chem.-Int. Edit.* **2016,** *55* (50), 15642-15645.
18. Roy, S. S.; Norcott, P.; Rayner, P. J.; Green, G. G. R.; Duckett, S. B., A Simple Route to Strong Carbon-13 NMR Signals Detectable for Several Minutes. *Chem.-Eur. J.* **2017,** *23* (44), 10496-10500.
19. Theis, T.; Ortiz, G. X.; Logan, A. W. J.; Claytor, K. E.; Feng, Y.; Huhn, W. P.; Blum, V.; Malcolmson, S. J.; Chekmenev, E. Y.; Wang, Q.; Warren, W. S., Direct and cost-efficient hyperpolarization of long-lived nuclear spin states on universal N-15(2)-diazirine molecular tags. *Sci. Adv.* **2016,** *2* (3), 7.
20. Stevanato, G.; Hill-Cousins, J. T.; Hakansson, P.; Roy, S. S.; Brown, L. J.; Brown, R. C. D.; Pileio, G.; Levitt, M. H., A Nuclear Singlet Lifetime of More than One Hour in Room-Temperature Solution. *Angew. Chem.-Int. Edit.* **2015,** *54* (12), 3740-3743.
21. Dumez, J. N., Perspective on long-lived nuclear spin states. *Molecular Physics*, 11.
22. Levitt, M. H., Long live the singlet state! *J. Magn. Reson.* **2019,** *306*, 69-74.
23. Sellies, L.; Reile, I.; Aspers, R.; Feiters, M. C.; Rutjes, F.; Tessari, M., Parahydrogen induced hyperpolarization provides a tool for NMR metabolomics at nanomolar concentrations. *Chem. Commun.* **2019,** *55* (50), 7235-7238.
24. Eshuis, N.; Hermkens, N.; van Weerdenburg, B. J. A.; Feiters, M. C.; Rutjes, F.; Wijmenga, S. S.; Tessari, M., Toward Nanomolar Detection by NMR Through SABRE Hyperpolarization. *J. Am. Chem. Soc.* **2014,** *136* (7), 2695-2698.
25. Iali, W.; Rayner, P. J.; Duckett, S. B., Using parahydrogen to hyperpolarize amines, amides, carboxylic acids, alcohols, phosphates, and carbonates. *Science Advance* **2018,** *4* (1).
26. Iali, W.; Rayner, P. J.; Alshehri, A.; Holmes, A. J.; Ruddlesden, A. J.; Duckett, S. B., Direct and indirect hyperpolarisation of amines using parahydrogen. *Chem. Sci.* **2018,** *9* (15), 3677-3684.
27. Gemeinhardt, M. E.; Limbach, M. N.; Gebhardt, T. R.; Eriksson, C. W.; Eriksson, S. L.; Lindale, J. R.; Goodson, E. A.; Warren, W. S.; Chekmenev, E. Y.; Goodson, B. M., "Direct" (13) C Hyperpolarization of (13) C-Acetate by MicroTesla NMR Signal Amplification by Reversible Exchange (SABRE). *Angew Chem Int Ed Engl* **2020,** *59* (1), 418-423.

28. Iali, W.; Roy, S. S.; Tickner, B.; Ahwal, F.; Kennerley, A. J.; Duckett, S. B., Hyperpolarising Pyruvate through Signal Amplification by Reversible Exchange (SABRE). *Angew. Chem.-Int. Edit.* **2019,** *58* (30), 10271-10275.
29. Durst, M.; Chiavazza, E.; Haase, A.; Aime, S.; Schwaiger, M.; Schulte, R. F., alpha-Trideuteromethyl 15N glutamine: A Long-Lived Hyperpolarized Perfusion Marker. *Magn. Reson. Med.* **2016,** *76* (6), 1900-1904.
30. Cudalbu, C.; Comment, A.; Kurdzesau, F.; van Heeswijk, R. B.; Uffmann, K.; Jannin, S.; Denisov, V.; Kirik, D.; Gruetter, R., Feasibility of in vivo N-15 MRS detection of hyperpolarized N-15 labeled choline in rats. *Phys. Chem. Chem. Phys.* **2010,** *12* (22), 5818-5823.
31. Gabellieri, C.; Reynolds, S.; Lavie, A.; Payne, G. S.; Leach, M. O.; Eykyn, T. R., Therapeutic target metabolism observed using hyperpolarized 15N choline. *J Am Chem Soc* **2008,** *130* (14), 4598-9.
32. Jagtap, A. P.; Kaltschnee, L.; Gloggler, S., Hyperpolarization of N-15-pyridinium and N-15-aniline derivatives by using parahydrogen: new opportunities to store nuclear spin polarization in aqueous media. *Chem. Sci.* **2019,** *10* (37), 8577-8582.
33. Harris, T.; Gamliel, A.; Uppala, S.; Nardi-Schreiber, A.; Sosna, J.; Gomori, J. M.; Katz-Brull, R., Long-lived N-15 Hyperpolarization and Rapid Relaxation as a Potential Basis for Repeated First Pass Perfusion Imaging - Marked Effects of Deuteration and Temperature. *Chemphyschem* **2018,** *19* (17), 2148-2152.
34. Atkinson, K. D.; Cowley, M. J.; Duckett, S. B.; Elliott, P. I. P.; Green, G. G. R.; Lopez-Serrano, J.; Khazal, I. G.; Whitwood, A. C., Para-Hydrogen Induced Polarization without Incorporation of Para-Hydrogen into the Analyte. *Inorg. Chem.* **2009,** *48* (2), 663-670.
35. Theis, T.; Truong, M. L.; Coffey, A. M.; Shchepin, R. V.; Waddell, K. W.; Shi, F.; Goodson, B. M.; Warren, W. S.; Chekmenev, E. Y., Microtesla SABRE Enables 10% Nitrogen-15 Nuclear Spin Polarization. *J. Am. Chem. Soc.* **2015,** *137* (4), 1404-1407.
36. Truong, M. L.; Theis, T.; Coffey, A. M.; Shchepin, R. V.; Waddell, K. W.; Shi, F.; Goodson, B. M.; Warren, W. S.; Chekmenev, E. Y., N-15 Hyperpolarization by Reversible Exchange Using SABRE-SHEATH. *J. Phys. Chem. C* **2015,** *119* (16), 8786-8797.
37. Colell, J. F. P.; Logan, A. W. J.; Zhou, Z.; Shchepin, R. V.; Barskiy, D. A.; Ortiz, G. X.; Wang, Q.; Malcolmson, S. J.; Chekmenev, E. Y.; Warren, W. S.; Theis, T., Generalizing, Extending, and Maximizing Nitrogen-15 Hyperpolarization Induced by Parahydrogen in Reversible Exchange. *The Journal of Physical Chemistry C* **2017,** *121* (12), 6626-6634.
38. Theis, T.; Truong, M.; Coffey, A. M.; Chekmenev, E. Y.; Warren, W. S., LIGHT-SABRE enables efficient in-magnet catalytic hyperpolarization. *J. Magn. Reson.* **2014,** *248*, 23-26.
39. Svyatova, A.; Skovpin, I. V.; Chukanov, N. V.; Kovtunov, K. V.; Chekmenev, E. Y.; Pravdivtsev, A. N.; Hovener, J. B.; Koptyug, I. V., N-15 MRI of SLIC-SABRE Hyperpolarized N-15-Labelled Pyridine and Nicotinamide. *Chem.-Eur. J.* **2019,** *25* (36), 8465-8470.
40. Pravdivtsev, A. N.; Yurkovskaya, A. V.; Zimmermann, H.; Vieth, H. M.; Ivanov, K. L., Enhancing NMR of insensitive nuclei by transfer of SABRE spin hyperpolarization. *Chemical Physics Letters* **2016,** *661*, 77-82.
41. Kidd, B. E.; Gesiorski, J. L.; Gemeinhardt, M. E.; Shchepin, R. V.; Kovtunov, K. V.; Koptyug, I. V.; Chekmenev, E. Y.; Goodson, B. M., Facile Removal of Homogeneous SABRE Catalysts for Purifying Hyperpolarized Metronidazole, a Potential Hypoxia Sensor. *The Journal of Physical Chemistry C* **2018,** *122* (29), 16848-16852.

42. Skovpin, I. V.; Svyatova, A.; Chukanov, N.; Chekmenev, E. Y.; Kovtunov, K. V.; Koptyug, I. V., N-15 Hyperpolarization of Dalfampridine at Natural Abundance for Magnetic Resonance Imaging. *Chem.-Eur. J.* **2019,** *25* (55), 12694-12697.
43. Torres, O.; Martín, M.; Sola, E., Labile N-Heterocyclic Carbene Complexes of Iridium. *Organometallics* **2009,** *28* (3), 863-870.
44. Fekete, M.; Bayfield, O.; Duckett, S. B.; Hart, S.; Mewis, R. E.; Pridmore, N.; Rayner, P. J.; Whitwood, A., Iridium(III) Hydrido N-Heterocyclic Carbene-Phosphine Complexes as Catalysts in Magnetization Transfer Reactions. *Inorganic Chemistry* **2013,** *52* (23), 13453-13461.
45. Mewis, R. E.; Atkinson, K. D.; Cowley, M. J.; Duckett, S. B.; Green, G. G. R.; Green, R. A.; Highton, L. A. R.; Kilgour, D.; Lloyd, L. S.; Lohman, J. A. B.; Williamson, D. C., Probing signal amplification by reversible exchange using an NMR flow system. **2014,** *52* (7), 358-369.
46. Jiang, W.; Lumata, L.; Chen, W.; Zhang, S.; Kovacs, Z.; Sherry, A. D.; Khemtong, C., Hyperpolarized 15N-pyridine Derivatives as pH-Sensitive MRI Agents. *Scientific Reports* **2015,** *5*, 9104.
47. Pyper, N. C., Theory of scalar relaxation of the second kind. II. *Molecular Physics* **1971,** *21* (6), 961-976.
48. Barskiy, D. A.; Shchepin, R. V.; Tanner, C. P. N.; Colell, J. F. P.; Goodson, B. M.; Theis, T.; Warren, W. S.; Chekmenev, E. Y., The Absence of Quadrupolar Nuclei Facilitates Efficient 13C Hyperpolarization via Reversible Exchange with Parahydrogen. *ChemPhysChem* **2017,** *18* (12), 1493-1498.
49. Kelly Iii, R. A.; Clavier, H.; Giudice, S.; Scott, N. M.; Stevens, E. D.; Bordner, J.; Samardjiev, I.; Hoff, C. D.; Cavallo, L.; Nolan, S. P., Determination of N-Heterocyclic Carbene (NHC) Steric and Electronic Parameters using the [(NHC)Ir(CO)2Cl] System. *Organometallics* **2008,** *27* (2), 202-210.
50. Kizaka-Kondoh, S.; Konse-Nagasawa, H., Significance of nitroimidazole compounds and hypoxia-inducible factor-1 for imaging tumor hypoxia. *Cancer Science* **2009,** *100* (8), 1366-1373.
51. Procissi, D.; Claus, F.; Burgman, P.; Koziorowski, J.; Chapman, J. D.; Thakur, S. B.; Matei, C.; Ling, C. C.; Koutcher, J. A., In vivo 19F Magnetic Resonance Spectroscopy and Chemical Shift Imaging of Tri-Fluoro-Nitroimidazole as a Potential Hypoxia Reporter in Solid Tumors. *Clinical Cancer Research* **2007,** *13* (12), 3738-3747.
52. Barskiy, D. A.; Shchepin, R. V.; Coffey, A. M.; Theis, T.; Warren, W. S.; Goodson, B. M.; Chekmenev, E. Y., Over 20% 15N Hyperpolarization in Under One Minute for Metronidazole, an Antibiotic and Hypoxia Probe. *J. Am. Chem. Soc.* **2016,** *138* (26), 8080-8083.
53. Shchepin, R. V.; Jaigirdar, L.; Theis, T.; Warren, W. S.; Goodson, B. M.; Chekmenev, E. Y., Spin Relays Enable Efficient Long-Range Heteronuclear Signal Amplification by Reversible Exchange. *J. Phys. Chem. C* **2017,** *121* (51), 28425-28434.
54. Shchepin, R. V.; Jaigirdar, L.; Chekmenev, E. Y., Spin–Lattice Relaxation of Hyperpolarized Metronidazole in Signal Amplification by Reversible Exchange in Micro-Tesla Fields. *J. Phys. Chem. C* **2018,** *122* (9), 4984-4996.
55. Kidd, B. E.; Gesiorski, J. L.; Gemeinhardt, M. E.; Shchepin, R. V.; Kovtunov, K. V.; Koptyug, I. V.; Chekmenev, E. Y.; Goodson, B. M., Facile Removal of Homogeneous SABRE Catalysts for Purifying Hyperpolarized Metronidazole, a Potential Hypoxia Sensor. *J. Phys. Chem C* **2018,** *122* (29), 16848-16852.

56. Richardson, P. M.; Iali, W.; Roy, S. S.; Rayner, P. J.; Halse, M. E.; Duckett, S. B., Rapid C-13 NMR hyperpolarization delivered from para-hydrogen enables the low concentration detection and quantification of sugars. *Chem. Sci.* **2019,** *10* (45), 10607-10619.